




Topological phases and collective modes in U(1) and SU(2) sectors of spin-orbit-coupled two-dimensional superfluid Fermi gases

Jeroen P. A. Devreese ^{1,2} Jacques Tempere ^{2,3} and Carlos A. R. Sá de Melo¹

¹*School of Physics, Georgia Institute of Technology, Atlanta, Georgia 30332, USA*

²*TQC, Departement Fysica, Universiteit Antwerpen, 2610 Antwerpen, Belgium*

³*Lyman Laboratory of Physics, Harvard University, Cambridge, Massachusetts 02138, USA*

 (Received 27 July 2019; revised 21 September 2021; accepted 24 January 2022; published 7 March 2022)

We study the emergence of finite-temperature topological phase transitions of the Berezinskii-Kosterlitz-Thouless type and the collective mode spectrum of two-dimensional Fermi gases in the presence of attractive s -wave interactions, spin-orbit coupling, and Zeeman fields. We show that neglecting the spin-dependent phase shift on the fermionic wave function misses an important point. Including this spin-dependent shift, we derive the effective low-energy and long-wavelength quantum action for independent (unlocked) phase fluctuations in the U(1) (charge) and SU(2) (spin) sectors and show that at least two phase transitions occur because charge and spin degrees of freedom are coupled due to the presence of spin-orbit and Zeeman fields. Furthermore, we demonstrate that vortex and antivortex excitations are characterized by two topological quantum numbers, corresponding to the quantized circulation of charge and spin velocities. Finally, we show that there are two collective modes in the superfluid phase at low temperatures which arise due to the coupling between sound and transverse-spin waves.

DOI: [10.1103/PhysRevA.105.033304](https://doi.org/10.1103/PhysRevA.105.033304)

I. INTRODUCTION

Recently, there has been a tremendous interest in topological phase transitions occurring in condensed-matter superconductors [1–3] and ultracold Fermi superfluids [4–8], where the interplay between pairing and spin-orbit coupling plays a crucial role. The classification of zero-temperature topological phases in superconductors was proposed [9,10] based on symmetry considerations of independent (quasi)particle Hamiltonians [11] for systems in which superconductivity is induced by the proximity effect in metals or in semiconductors with strong spin-orbit coupling. In this case, a mean-field description that neglects fluctuations is generally sufficient [12–15]. In ultracold Fermi superfluids, the situation is quite different because it is possible to create an artificial strong spin-orbit coupling [16,17] directly in the superfluid with controllable pairing interactions [18,19]. This implies that the order parameter for superfluidity in ultracold atoms is a self-consistent quantity and that changing the interactions from weak to strong requires an analysis beyond mean-field theory [20,21]. In particular, if one wants to study topological superfluidity in two-dimensional systems at nonzero temperature it is essential to include the effects of phase fluctuations [22–24].

In previous work discussing the effects of spin-orbit coupling in two-dimensional Fermi superfluids [4–8], including our own work [25,26], the phase shift of the fermions was assumed to be spin independent so that only charge degrees of freedom were included, that is, a total U(1) phase. However, this assumption ignores the existence of a spin-dependent phase shift on the wave function of individual fermions. In contrast, we show that the inclusion of this spin degree of

freedom, the SU(2) phase, cannot be ignored when spin-orbit coupling is present and may lead to new physics. In particular, the inclusion of this spin degree of freedom leads to an XY spin stiffness and an additional finite-temperature phase transition of the Berezinskii-Kosterlitz-Thouless (BKT) universality class [27,28]. Note that this is a phase transition induced by the proliferation of topological defects such as vortices and antivortices, but it is not a transition between different topological phases that have different global topological invariants.

In this paper, we derive the quantum effective action including U(1) and SU(2) phase fluctuations for contact s -wave interactions, spin-orbit coupling, and Zeeman fields. The resulting action contains phase stiffnesses in the U(1), SU(2), and U(1)×SU(2) sectors. The SU(2) and the U(1)×SU(2) phase stiffnesses emerge due to spin-orbit coupling and Zeeman fields and affect not only collective modes, but also topological excitations such as vortices and antivortices. An analysis of the U(1) and SU(2) vortices or antivortices and their unbinding reveals the existence of at least two finite-temperature topological phase transitions of the BKT type. Furthermore, in the superfluid phase at low temperatures, the low-energy and long-wavelength collective excitations are no longer the pure sound mode found in the U(1) sector; instead there are two eigenmodes resulting from the coupling between sound and transverse-spin waves originated from the U(1) and SU(2) sectors, respectively.

This paper is structured as follows. We start by defining the system through its Hamiltonian in Sec. II using a general spin-orbit coupling. The U(1) and SU(2) phase fields are introduced in Sec. III. The effective action for these phase fields

is expanded to second order, leading to a description of the coupled phase fluctuations in Sec. IV. We particularize the general spin-orbit coupling to the equal Rashba-Dresselhaus case relevant to the ultracold atomic gases and discuss the results in Sec. V. We make some final remarks in Sec. VI and state our conclusions in Sec. VII. Details of the calculations are given in the Appendices, to keep the readability of the paper.

II. SYSTEM HAMILTONIAN

In order to describe the physics outlined above, we begin by defining our unit system, where we set $\hbar = 2m = E_F = 1$, with m and E_F the atom mass and the Fermi energy, respectively. This means that the momentum scale is the Fermi momentum $k_F = \sqrt{2mE_F/\hbar^2} = 1$ and that the velocity scale is $v_F = \hbar k_F/m = 2$. We begin our analysis from the Hamiltonian density

$$\mathcal{H}(r) = \mathcal{H}_0(r) + \mathcal{H}_{\text{SO}}(r) + \mathcal{H}_I(r), \quad (1)$$

where $r = (\mathbf{r}, \tau)$ is a three-vector representing the particle position $\mathbf{r} = (x, y)$ in two spatial dimensions and imaginary time τ . The independent-particle contribution without spin-orbit coupling is

$$\mathcal{H}_0(r) = \sum_{s,s'} \psi_{rs}^\dagger [\hat{K}_s \delta_{ss'} - (h_z \sigma_z)_{ss'}] \psi_{rs'}, \quad (2)$$

where $\hat{K}_s = -\nabla_{\mathbf{r}}^2 - \mu_s$ is the kinetic energy of a fermion with spin $s = (\uparrow, \downarrow)$ measured with respect to its chemical potential μ_s . Here h_z plays the role of a Zeeman field along the z axis, while ψ_{rs}^\dagger and ψ_{rs} are fermionic fields and σ_i represents the i th $[(x, y, z)]$ Pauli matrix.

The second term in Eq. (1) is given by

$$\mathcal{H}_{\text{SO}}(r) = - \sum_{ss'} \psi_{rs}^\dagger [2\alpha \hat{k}_x (\sigma_y)_{ss'} - 2\gamma \hat{k}_y (\sigma_x)_{ss'}] \psi_{rs'} \quad (3)$$

and describes spin-orbit coupling. Here the momentum operator is $\hat{k}_\eta = -i(\partial/\partial\eta)$, with $\eta = \{x, y\}$, while the parameters $\alpha = (v_R + v_D)/2$ and $\gamma = (v_R - v_D)/2$ are the sum and difference of the Rashba [29] and Dresselhaus [30] couplings v_R and v_D , respectively. Notice in Eq. (3) that the spin-orbit coupling is in general two dimensional, and thus we can study spin-orbit couplings from the limit of the extremely anisotropic equal Rashba-Dresselhaus (ERD) case ($v_R = v_D = v$, $\alpha = v$, and $\gamma = 0$) found easily in the context of ultracold atoms to the limit of Rashba-only case ($v_D = 0$, $v_R \neq 0$, and $\alpha = \gamma = v_R/2$) or Dresselhaus-only case ($v_D \neq 0$, $v_R = 0$, and $\alpha = -\gamma = v_D/2$) encountered in typical condensed-matter systems.

The terms involving α and γ in Eq. (1) can be interpreted as the components of the transverse field operator $\hat{\mathbf{h}}_\perp = (\hat{h}_x, \hat{h}_y)$, with $\hat{h}_x = -2\gamma \hat{k}_y$ and $\hat{h}_y = 2\alpha \hat{k}_x$. The corresponding matrix for the spin-orbit Hamiltonian density can be written as $-\hat{h}_\perp \sigma^- - \hat{h}_\perp^* \sigma^+$, where $\hat{h}_\perp = \hat{h}_x + i\hat{h}_y$ is the complex transverse field operator and $\sigma^\pm = (\sigma_x \pm i\sigma_y)/2$ is the spin raising (+) or lowering (−) operator. The last term in Eq. (1) represents the interaction Hamiltonian density

$$\mathcal{H}_I(r) = -g \psi_{r\uparrow}^\dagger \psi_{r\downarrow}^\dagger \psi_{r\downarrow} \psi_{r\uparrow}, \quad (4)$$

which describes fermions interacting via an attractive s -wave contact interaction with strength $g > 0$.

III. EFFECTIVE ACTION FOR THE PHASE FIELDS

To obtain the effective action, we begin from the partition function $\mathcal{Z} = \int \mathcal{D}\psi^\dagger \mathcal{D}\psi \exp[-S(\psi^\dagger, \psi)]$, where the starting action is

$$S(\psi^\dagger, \psi) = \int dr \left[\sum_s \psi_{rs}^\dagger \frac{\partial}{\partial \tau} \psi_{rs} + \mathcal{H}(r) \right]. \quad (5)$$

To keep the readability of the paper, we defer details of the derivation to Appendix A. Thus, below we only outline some steps and discuss the physical meaning of the resulting terms.

First, we write the contribution of the interaction Hamiltonian density $\mathcal{H}_I(r)$ to the action in terms of a Hubbard-Stratonovich transformation involving complex fields Δ_r^* and Δ_r as

$$\mathcal{S}_{\text{int}} = \int dr \left(\psi_{r,\uparrow}^\dagger \psi_{r,\downarrow}^\dagger \Delta_r + \psi_{r,\downarrow} \psi_{r,\uparrow} \Delta_r^\dagger - \frac{\Delta_r^\dagger \Delta_r}{g} \right). \quad (6)$$

Second, we perform a spin-dependent gauge transformation in the Fermi fields by writing

$$\psi_{rs} \rightarrow \tilde{\psi}_{rs} e^{i\phi_s(r)}, \quad (7)$$

$$\psi_{rs}^\dagger \rightarrow \tilde{\psi}_{rs}^\dagger e^{-i\phi_s(r)}, \quad (8)$$

$$\Delta_r \rightarrow \tilde{\Delta}_r e^{i\phi_\uparrow(r) + i\phi_\downarrow(r)} = \tilde{\Delta}_r e^{i\phi_\pm}. \quad (9)$$

It is important to emphasize that the phase $\phi_s(r)$ is spin dependent, as this has profound consequences on the resulting effective action. The phase $\phi_+(r) = \phi_\uparrow(r) + \phi_\downarrow(r)$ characterizes the U(1) charge sector of the particle-particle channel. However, there is also an associated SU(2) spin-flip phase $\phi_-(r) = \phi_\uparrow(r) - \phi_\downarrow(r)$ in the particle-hole sector of the off-diagonal elements of $\mathcal{H}_{\text{SO}}(r)$.

To see this explicitly, it is more convenient to write the spin-orbit Hamiltonian density $\mathcal{H}_{\text{SO}}(r) = -\psi_{r\uparrow}^\dagger \hat{h}_\perp^* \psi_{r\downarrow} - \psi_{r\downarrow}^\dagger \hat{h}_\perp \psi_{r\uparrow}$ in terms of the spin operators $S_+(r) = \psi_{r\uparrow}^\dagger \psi_{r\downarrow}$ and $S_-(r) = \psi_{r\downarrow}^\dagger \psi_{r\uparrow}$, yielding

$$\mathcal{H}_{\text{SO}} = -\hat{h}_\perp^* S_+(r) - \hat{h}_\perp S_-(r) + [\hat{h}_\perp^*, \psi_{r\uparrow}^\dagger] \psi_{r\downarrow} + [\hat{h}_\perp, \psi_{r\downarrow}^\dagger] \psi_{r\uparrow}. \quad (10)$$

Under the spin-dependent gauge transformation the spin-flip operators transform as $\tilde{S}_+(r) = S_+(r) e^{i\phi_-(r)}$ and $\tilde{S}_-(r) = S_-(r) e^{-i\phi_-(r)}$, where $\phi_-(r) = \phi_\uparrow(r) - \phi_\downarrow(r)$ plays the role of an SU(2) transverse-spin phase. Hence, when spin-orbit coupling is present, the phases $\phi_+(r)$ and $\phi_-(r)$ both play an important role in the final effective action obtained below.

After integration over the Fermi fields $\tilde{\psi}_{rs}$ and $\tilde{\psi}_{rs}^\dagger$, the partition function \mathcal{Z} is a functional of the phases $\phi_\uparrow(r)$ and $\phi_\downarrow(r)$ and of the amplitude $|\Delta_r|$. However, since we expect phase fluctuations to provide the dominant contributions in two dimensions, we assume that the order parameter is uniform in space and imaginary time by setting $|\Delta_r| = |\Delta|$. Performing a Fourier transformation, we obtain the partition

function $\mathcal{Z} = \int \mathcal{D}\phi_\uparrow \phi_\downarrow \exp\{-S_{\text{eff}}[\phi_\uparrow, \phi_\downarrow]\}$, where the action

$$S_{\text{eff}} = -\frac{1}{2} \text{Tr} \left\{ \ln \left[\beta \begin{pmatrix} \mathbb{A}_+ & \mathbb{B}_+ \\ \mathbb{B}_- & \mathbb{A}_-^* \end{pmatrix} \right] \right\} - \frac{\beta L^2 |\Delta|^2}{g} + S_x, \quad (11)$$

with β the inverse temperature and L^2 the area of the two-dimensional system. The traces are taken over $k = (\mathbf{k}, i\omega_n)$, where \mathbf{k} is the fermionic wave vector and $\omega_n = (2n+1)\pi/\beta$ is the fermionic Matsubara frequency. The 2×2 matrices \mathbb{A}_+ and \mathbb{A}_-^* describe energies in the particle-hole sector, while matrices \mathbb{B}_+ and \mathbb{B}_- describe energies in the particle-particle sector, and S_x is independent of interactions. Expressions for all these terms can be found in Appendix A.

IV. COUPLED PHASE FLUCTUATIONS

An expansion in ϕ_s results in an effective action $S_{\text{eff}} = S_{\text{SP}} + S_{\text{fl}}$, where the first term is the saddle-point contribution leading to the thermodynamic potential

$$\Omega_{\text{SP}} = \sum_{\mathbf{k}} \left(\frac{-1}{2\beta} \sum_{i=\pm} \ln[2 + 2 \cosh(\beta E_i)] + \xi_{\mathbf{k}} \right) - \frac{L^2 |\Delta|^2}{g}. \quad (12)$$

Here

$$E_{\pm} = \sqrt{[E_S(\mathbf{k}) \pm |\mathbf{h}_{\text{eff}}(\mathbf{k})|]^2 + |\Delta_T(\mathbf{k})|^2} \quad (13)$$

are the quasiparticle energies, $E_S(\mathbf{k}) = \sqrt{\xi_{\mathbf{k}}^2 + |\Delta_S(\mathbf{k})|^2}$ is the energy associated with the order parameter component $\Delta_S(\mathbf{k}) = |\Delta| h_z / |\mathbf{h}_{\text{eff}}(\mathbf{k})|$ in the singlet sector, and $\Delta_T(\mathbf{k}) = |\Delta| h_{\perp}^* / |\mathbf{h}_{\text{eff}}(\mathbf{k})|$ is the order parameter component in the triplet sector induced by spin-orbit coupling, where $\mathbf{h}_{\text{eff}}(\mathbf{k}) = [h_x(\mathbf{k}), h_y(\mathbf{k}), h_z]$ plays the role of an effective momentum-dependent Zeeman field. Finally, we substitute the interaction g by the two-body binding energy E_b via the Lippmann-Schwinger relation

$$\frac{1}{g} = - \int \frac{d\mathbf{k}}{(2\pi)^2} \frac{1}{2k^2 + E_b} \quad (14)$$

in two spatial dimensions.

The second term in the expansion is the phase-fluctuation action, written in terms of the phases $\phi_+(r)$ in the U(1) sector and $\phi_-(r)$ in the SU(2) sector as

$$S_{\text{fl}} = \frac{1}{2} \int dx dy d\tau (\kappa_{mn} \partial_\tau \phi_m \partial_\tau \phi_n + \rho_{mn}^{\nu\lambda} \partial_\nu \phi_m \partial_\lambda \phi_n), \quad (15)$$

where the indices m, n take values $\{+, -\}$, ∂_τ indicates the partial imaginary-time derivative, and ∂_ν and ∂_λ describe partial spatial derivatives with ν or λ being $\{x, y\}$. Details of the derivation can be found in Appendix B. The detailed microscopic expressions for κ_{mn} and for $\rho_{mn}^{\nu\lambda}$ are discussed in Appendix C.

The quantum action shown in Eq. (15) describes two coupled systems: One is the charge sector labeled by $\{++\}$, the other is the spin sector labeled by $\{--\}$, and their coupling is labeled by $\{+-\}$, $\{-+\}$. The gradients $\partial_\lambda \phi_+(r)$ and $\partial_\lambda \phi_-(r)$ play the roles of the superfluid velocity and of the spatial derivative of the transverse magnetization, respectively. Notice that the quantum action reveals a drag effect between charge and spin currents due to the coupling between $\partial_\nu \phi_+$ and $\partial_\lambda \phi_-$ induced by the presence of spin-orbit coupling.

The coupling term is very important in the analysis of the collective phase modes that will be discussed later.

The coefficient κ_{++} describes the compressibility of the U(1) sector associated with $\phi_+(r)$ only; κ_{--} reflects the compressibility of the transverse-spin SU(2) sector associated with $\phi_-(r)$ only; κ_{+-} and κ_{-+} are compressibilities that reveal the coupling between the two sectors. In the limit where the spin-orbit coupling is zero, κ_{+-} , κ_{-+} , κ_{--} vanish and only the U(1) sector corresponding to the superfluid component remains. Furthermore, for nonzero spin-orbit coupling, only the κ_{++} term contributes when the phases are locked, that is, when $\phi_-(r) = 0$. The tensor $\rho_{mn}^{\nu\lambda}$ represents a generalized phase stiffness. Again, in the limit of zero spin-orbit coupling the phase-stiffness components $\rho_{+-}^{\nu\lambda}$, $\rho_{-+}^{\nu\lambda}$, $\rho_{--}^{\nu\lambda}$ vanish and only $\rho_{++}^{\nu\lambda} = \rho_{++} \delta_{\nu\lambda}$ survives in the U(1) sector corresponding to a superfluid density tensor that is isotropic. In addition, when the spin-orbit coupling is nonzero and the phases are locked with $\phi_-(r) = 0$, only the U(1) sector contributes to the action, but the superfluid density tensor $\rho_{++}^{\nu\lambda}$ is anisotropic. The microscopic expressions for κ_{mn} and for $\rho_{mn}^{\nu\lambda}$ are found in Appendix C.

Next we rotate (x, y) into (\bar{x}, \bar{y}) such that the phase stiffness tensor is diagonal in spatial coordinates, with elements $\rho_{mn}^{\bar{x}\bar{x}}$ and $\rho_{mn}^{\bar{y}\bar{y}}$. Finally, we rescale $\bar{x} = [\rho_{mn}^{\bar{x}\bar{x}}]^{1/2} \bar{x}$ and $\bar{y} = [\rho_{mn}^{\bar{y}\bar{y}}]^{1/2} \bar{y}$ to make the phase stiffness tensor isotropic in space, $\bar{\rho}_{mn} = [\rho_{mn}^{\bar{x}\bar{x}} \otimes \rho_{mn}^{\bar{y}\bar{y}}]^{1/2}$. This turns the action from Eq. (15) into

$$S_{\text{fl}} = \frac{1}{2} \int d\bar{x} d\bar{y} d\tau (\bar{\kappa}_{mn} \partial_\tau \phi_m \partial_\tau \phi_n + \bar{\rho}_{mn} \partial_\nu \phi_m \partial_\nu \phi_n) \quad (16)$$

in the coordinate system (\bar{x}, \bar{y}) . In Eq. (16) the renormalized compressibility matrix elements are $\bar{\kappa}_{mn} = \bar{\rho}_{mn} \otimes \kappa_{mn}$, where \otimes represents direct product. Stability requires that $\bar{\kappa}_{mn}$ and $\bar{\rho}_{mn}$ are matrices with positive eigenvalues, that is, the traces and the determinants of $\bar{\kappa}_{mn}$ and $\bar{\rho}_{mn}$ are positive.

In thermodynamic equilibrium the phase fields are independent of time τ and thus only the spatial part of the action is important. Since the phases $\phi_+(x, y)$ and $\phi_-(x, y)$ in the original coordinates (x, y) are defined modulo 2π , vortex solutions associated with these phase fields have to satisfy the quantization of circulation $\oint_C \nabla \phi_m(\mathbf{r}) \cdot d\mathbf{l} = 2\pi Q_m$, where Q_m is the topological index characterizing the vorticity, that is, the topological charge. Since Q_m is a scalar, any conformal deformation of $\phi_m(\mathbf{r})$ produces the same topological charge; thus in the transformed coordinates (\bar{x}, \bar{y}) the circulation quantization is written as $\oint_C \bar{\nabla} \phi_m(\bar{\mathbf{r}}) \cdot d\bar{\mathbf{l}} = 2\pi Q_m$.

The topological excitations of the action in Eq. (16) are vortices with topological indices (Q_+, Q_-) . A phase transition occurs at the critical temperature $T_{++} = \frac{\pi}{2} \bar{\rho}_{++}$ in the charge sector when charge vortex ($Q_+ = +1, Q_- = 0$) and antivortex ($Q_+ = -1, Q_- = 0$) unbind. Similarly, a phase transition occurs at $T_{--} = \frac{\pi}{2} \bar{\rho}_{--}$ in the spin sector when the spin vortex ($Q_+ = 0, Q_- = +1$) and antivortex ($Q_+ = 0, Q_- = -1$) unbind. An illustration of the vortex-antivortex pairs in the two sectors is shown in Fig. 1. We also mention in passing the possibility of another transition when there is vorticity in both charge and spin sectors. Such transitions correspond to unbinding of the composite vortex ($Q_+ = +1, Q_- = +1$) and composite antivortex ($Q_+ = -1, Q_- = -1$) or unbinding of the composite vortex ($Q_+ = +1, Q_- = -1$) and

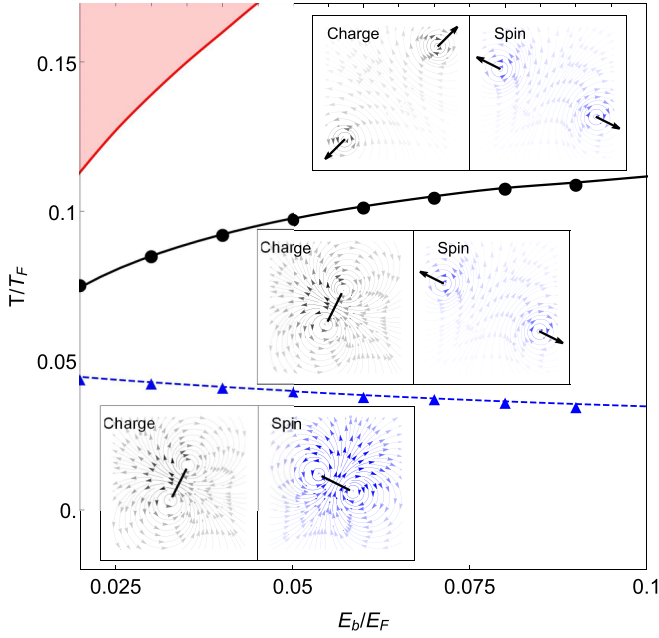


FIG. 1. Schematic illustration of the two BKT transitions, related to unbinding of vortex-antivortex pairs in the spin sector and the charge sector, consecutively, as the temperature T/T_F is increased. The blue triangles and dashed line represent the BKT temperature for the spin sector and the black circles and curve represent the transition temperature for the charge sector, both for $v/\tilde{v}_F = 0.6$ and $h_z/E_F = 0.01$. In the shaded area, $|\Delta| = 0$.

composite antivortex ($Q_+ = -1, Q_- = +1$). For instance, when the off-diagonal stiffness $\bar{\rho}_{+-}$ is positive but sufficiently small such that $\bar{\rho}_{+-} < \max\{\bar{\rho}_{++}, \bar{\rho}_{--}\}/2$ while still satisfying the stability condition $|\bar{\rho}_{+-}| < [\bar{\rho}_{++}\bar{\rho}_{--}]^{1/2}$ for the positivity of $\bar{\rho}_{mn}$, this new phase does not emerge, at least in the ERD case discussed below and for the parameters used below.

The phase transition in the SU(2) spin channel will lead to a direct signature in the spin susceptibility. This quantity has been measured experimentally in strongly interacting Fermi gases by various techniques, using the equation of state [31], speckle imaging [32], and radio-frequency dressing [33]. In addition, vortex rotation can be detected by Bragg spectroscopy [34,35], and spin-dependent Bragg spectroscopy could be used to detect the SU(2) channel vortices. Vortex-antivortex unbinding has been detected through interferometric [36,37] or density techniques [38] that can be made spin selective [39].

V. RESULTS AND DISCUSSION FOR THE ERD CASE

All the analytical results discussed above are valid for general two-dimensional spin-orbit couplings, that is, for any linear combination of Rashba and Dresselhaus contributions. However, in the remainder of this paper, we focus on the equal Rashba-Dresselhaus case $v_R = v_D = v$, which is relevant for ultracold fermions. In Fig. 2, we show the behavior of T_{++} and T_{--} (in units $T_F = E_F/k_B$) versus E_b and Zeeman field h_z for fixed values of the ERD spin-orbit coupling parameter v . In Fig. 2(a), $h_z/E_F = 0.01$ is small in comparison to v/\tilde{v}_F with $\tilde{v}_F = v_F/2$, where the system is nearly Galilean

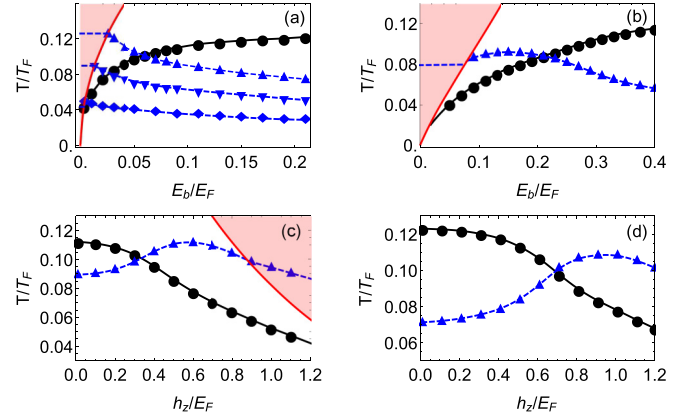


FIG. 2. The BKT transition temperatures T_{++} for the charge sector and T_{--} for the spin sector. (a) Temperatures T_{++} (circles, $v/\tilde{v}_F = 0.8$) and T_{--} (diamonds, $v/\tilde{v}_F = 0.6$; squares, $v/\tilde{v}_F = 0.8$; and triangles, $v/\tilde{v}_F = 1.0$) are shown as a function of E_b for $h_z/E_F = 0.01$. The curves for T_{--} scale approximately as v^2 . (b) Temperatures T_{++} (circles) and T_{--} (squares) are shown as a function of E_b at $h_z/E_F = 0.6$, $v/\tilde{v}_F = 0.8$. (c) and (d) Temperatures T_{++} (circles) and T_{--} (triangles) are shown for $v/\tilde{v}_F = 1.0$ as a function of h_z at (c) $E_b/E_F = 0.1$ and (d) $E_b/E_F = 0.25$. The shaded area above the red solid line represents the region where the order parameter $|\Delta| = 0$. Curves connecting symbols are a guide for the eye.

invariant. The temperature T_{++} in the charge sector and the boundary of the shaded area where $|\Delta| = 0$ is largely insensitive to the values of v/\tilde{v}_F . However, T_{--} increases with growing values of v/\tilde{v}_F , reflecting the mounting importance of the spin sector and the induced triplet component of the order parameter. Within the superfluid region, notice that T_{--} decreases as a function of the binding energy. The reason is that larger binding energies favor spin-singlet pairing, which in turn suppresses longitudinal spin fluctuations (z axis). Due to the noncommuting nature of the spin operators, this will enhance the transverse-spin fluctuations (xy plane), thereby reducing the transverse-spin stiffness. In Fig. 2(b), $h_z/E_F = 0.6$ is comparable to $v/\tilde{v}_F = 0.8$. The effect of an increase in h_z is detrimental for the quantities related to the charge sector (T_{++} and the temperature where $|\Delta| = 0$ are reduced), but it enhances the importance of the spin sector in the triplet channel (T_{--} increases), as can be more clearly seen in Figs. 2(c) and 2(d). As h_z approaches the pair-breaking $|\Delta| = 0$ region, T_{--} becomes suppressed by the closing of the gap, giving rise to a maximum as a function of h_z . As can be seen in Figs. 2(a)–2(c), the T_{--} curve crosses into the region where $|\Delta| = 0$. Due to spin-orbit coupling, the spin sector in our system has a spin stiffness that is nonzero even when the superfluid order parameter is zero. Above the line $|\Delta| = 0$, the spin stiffness is independent of E_b , but it still depends on v/\tilde{v} and h_z . When $|\Delta| > 0$, the transition temperature is modified by the coupling to the superfluid sector and thus becomes dependent on E_b .

In Fig. 3, we show the phase stiffnesses in the charge ($\bar{\rho}_{++}$), spin ($\bar{\rho}_{+-}$), and mixed ($\bar{\rho}_{+-} = \bar{\rho}_{-+}$) sectors, illustrating their universal jumps at the vortex-antivortex unbinding critical temperatures T_{++} and T_{--} in the charge and spin sectors, respectively. Notice that $\bar{\rho}_{+-}$ jumps to zero always

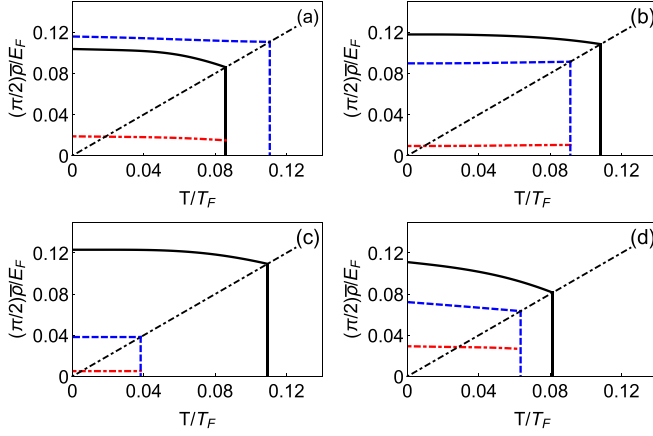


FIG. 3. Phase stiffnesses $\bar{\rho}_{mn}$ are shown as a function of T/T_F for several values of the binding energy E_b (in units E_F), the SOC strength v (in units \tilde{v}_F) and h_z (in units E_F): (a) $h_z = 0.5$, $v = 1$, and $E_b = 0.1$; (b) $h_z = 0.5$, $v = 1$, and $E_b = 0.2$; (c) $h_z = 0.3$, $v = 0.6$, and $E_b = 0.15$; and (d) $h_z = 0.5$, $v = 0.6$, and $E_b = 0.15$. The stiffnesses corresponding to charge ($\bar{\rho}_{++}$) and spin ($\bar{\rho}_{--}$) sectors are shown by the black solid and the blue dashed curves, respectively. The red dash-dotted line shows $\bar{\rho}_{+-}$. The phase stiffnesses are scaled by $\pi/2$, so the intersect with the temperature (black dash-dotted thin line) indicates the critical BKT temperature corresponding to each curve, where the phase stiffness drops discontinuously to zero.

at the $\min\{T_{--}, T_{++}\}$. The terms involving $\bar{\rho}_{+-}$ and $\bar{\rho}_{-+}$ describe a charge-spin or spin-charge drag effect induced by the simultaneous presence of spin-orbit coupling and Zeeman fields.

To study the collective modes, we take into account the spatial and temporal dependences of the phase fields $\phi_m(\mathbf{r}, \tau)$ and work in momentum and frequency space. The analytic continuation $i\omega_n \rightarrow \omega + i\delta$ leads to

$$S_{\text{fl}} = \frac{1}{2} \sum_{\mathbf{q}, \omega} [\omega^2 \bar{\kappa}_{mn} - \bar{\mathbf{q}}^2 \bar{\rho}_{mn}] \phi_m(-\mathbf{q}, \omega) \phi_n(\mathbf{q}, \omega). \quad (17)$$

There are two eigenmodes. Only when $\bar{\rho}_{+-} = \bar{\rho}_{-+} = 0$ there are pure charge (sound-wave) and pure spin (transverse-spin-wave) modes. In this case, the charge mode has dispersion $\omega^2(\mathbf{q}) = \bar{c}_+^2 \bar{\mathbf{q}}^2$, where $\bar{c}_+ = [\bar{\rho}_{++}/\bar{\kappa}_{++}]^{1/2}$ plays the role of the sound velocity, and the spin mode has dispersion $\omega^2(\mathbf{q}) = \bar{c}_-^2 \bar{\mathbf{q}}^2$, where $\bar{c}_- = [\bar{\rho}_{--}/\bar{\kappa}_{--}]^{1/2}$ plays the role of the transverse-spin-wave velocity. However, for nonzero spin-orbit coupling and Zeeman fields, the sound- and spin-wave modes are always coupled, leading to dispersions $\omega_1^2 = \bar{c}_1^2 \bar{\mathbf{q}}^2$ with propagation speed $\bar{c}_1^2 = \bar{c}_s^2 + (\bar{c}_d^4 + \bar{c}_{+-}^4)^{1/2}$ for the higher-frequency mode and $\omega_2^2 = \bar{c}_2^2 \bar{\mathbf{q}}^2$ with propagation speed $\bar{c}_2^2 = \bar{c}_s^2 - (\bar{c}_d^4 + \bar{c}_{+-}^4)^{1/2}$ for the lower-frequency mode. Here the squared-sum speed is $\bar{c}_s^2 = (\bar{c}_+^2 + \bar{c}_-^2)/2$, the squared-difference speed is $\bar{c}_d^2 = (\bar{c}_+^2 - \bar{c}_-^2)/2$, and the cross speed is $\bar{c}_{+-}^4 = \bar{\rho}_{+-}\bar{\rho}_{-+}/\bar{\kappa}_{++}\bar{\kappa}_{--}$. The dispersions are given in transformed momentum coordinates (\bar{q}_x, \bar{q}_y) , where the action is isotropic. A return to the original momentum coordinates (q_x, q_y) requires undoing the scaling and rotation transformations, implemented earlier in real space. In the original coordinates, the collective mode velocities $c_{1,x}$ and $c_{2,x}$ in the x direction are different from $c_{1,y}$ and $c_{2,y}$ in the

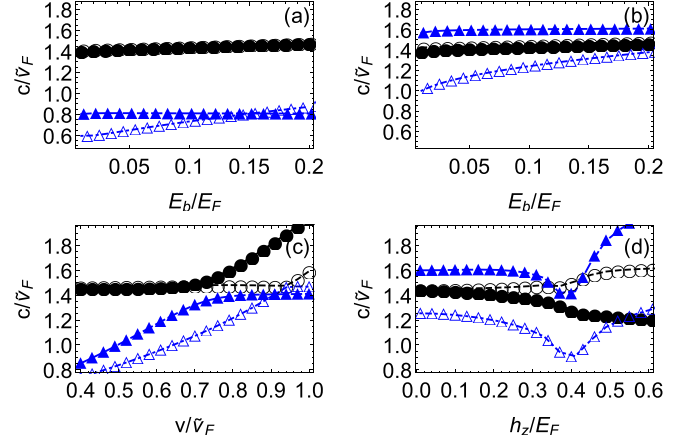


FIG. 4. Collective mode velocities (in units $\tilde{v}_F = v_F/2$) are shown for the first mode $c_{1,x}$ (closed black circles) and $c_{1,y}$ (open black circles) and for the second mode $c_{2,x}$ (closed blue triangles) and $c_{2,y}$ (open blue triangles). Collective mode velocities are plotted as a function of the binding energy for (a) smaller spin-orbit coupling ($v/\tilde{v}_F = 0.4$) and (b) larger spin-orbit coupling ($v/\tilde{v}_F = 0.8$), at $h_z/E_F = 0.1$. (c) At fixed $E_b/E_F = 0.15$ and Zeeman field $h_z/E_F = 0.3$, the velocities are shown as a function of the ERD spin-orbit coupling v/\tilde{v}_F . (d) The effect of increasing h_z is shown at $E_b/E_F = 0.1$ and $v/\tilde{v}_F = 0.8$.

y direction, reflecting the anisotropy of the ERD spin-orbit coupling. In the case of pure Rashba or Dresselhaus spin-orbit coupling, the collective mode velocities are isotropic; however, any nontrivial linear combination of the two terms will always lead to anisotropies. In Fig. 4, we show the collective mode velocities at $T/T_F = 0.01$. In Figs. 4(a) and 4(b), they are shown as a function of E_b/E_F at $h_z/E_F = 0.1$, for smaller [Fig. 4(a)] and larger [Fig. 4(b)] spin-orbit coupling. In this regime, the charge and spin modes are weakly coupled: The first mode (black circles) has dominantly charge character, whereas the second mode (blue triangles) has predominantly spin character. In the regions of the phase diagram where $T_{++} > T_{--}$, the collective modes are a mix of sound and spin waves for $T < T_{--}$, but for $T_{--} < T < T_{++}$ where $\bar{\rho}_{--}$ and $\bar{\rho}_{+-}, \bar{\rho}_{-+}$ have vanished, there is only the sound mode left. Conversely, in regions where $T_{++} < T_{--}$, the collective modes are a mix of sound and spin waves for $T < T_{++}$, but for $T_{++} < T < T_{--}$ where $\bar{\rho}_{++}$ and $\bar{\rho}_{+-}, \bar{\rho}_{-+}$ have vanished, there is only the spin-wave mode left. This shows that for fixed binding energy, spin-orbit coupling, and Zeeman fields, but changing temperatures, one can probe one or two collective modes.

For the domain of binding energies E_b shown, the first mode velocity is largely insensitive to changes in E_b or v and is nearly isotropic, whereas the second mode is visibly anisotropic and its velocity increases as a function of v . Moreover, $c_{2,y}$ (open blue triangles) is more sensitive to E_b than $c_{2,x}$ (closed blue triangles). Figure 4(c) shows the influence of the spin-orbit-coupling strength on the modes, revealing two avoided crossings. In the x direction the first (second) mode, shown with closed circles (closed triangles), is mostly a charge (spin) mode before the avoided crossing, turning into a predominantly spin (charge) mode afterward. A similar effect

happens in the y direction. In Fig. 4(d), with increasing h_z , the excitation spectrum of the superfluid changes from a regime with an indirect gap ($h_z/E_F \lesssim 0.4$) to a regime with a node ($h_z/E_F \gtrsim 0.4$) which affects the curvature and slopes of all collective mode velocities.

VI. FINAL REMARKS

We would like to emphasize that the theory described in this paper includes only phase fluctuations, which works well for values of $E_b/E_F \lesssim 0.4$ [26]. For larger values of the binding energy it is necessary to include also fluctuations of the order parameter modulus, given that the coupling between the phase and modulus increases from the BCS to the Bose regime as in the three-dimensional case. These corrections modify the chemical potential, the sound velocity, and the critical temperature as the Bose regime is approached. The study of these effects is left for later investigation.

VII. CONCLUSION

In conclusion, we have shown that spin-orbit-coupled Fermi gases in two dimensions may exhibit two distinct topological phase transitions belonging to the BKT universality class. The first one occurs in the U(1) charge sector and is related to the phase sum of both spin components, while the second one occurs in the SU(2) spin sector and is related to the phase difference between the spin components. We characterized the critical temperatures for these transitions in various regimes, as well as the collective modes at low temperature. Our results suggest that spin-orbit coupling introduces additional topological phases and collective excitations as a result of the interplay between charge and spin degrees of freedom, relevant not only for superfluid Fermi gases but also for solid-state superconductors.

ACKNOWLEDGMENTS

J.P.A.D. thanks E. Vermeyen for stimulating discussions. We acknowledge financial support from ARO (Grant No. W911NF-09-1-0220), from the University Research Fund (BOF) of the University of Antwerp, and from the Research Foundation-Flanders (FWO-Vlaanderen) via a postdoctoral fellowship (J.P.A.D.) and Grant No. G.0429.15N.

APPENDIX A: DERIVATION OF THE EFFECTIVE ACTION FOR THE PHASE FIELDS

The Hamiltonian $\mathcal{H}(r)$ defined in Eq. (1) leads straightforwardly to the action functional $\mathcal{S} = \mathcal{S}_{\text{free}} + \mathcal{S}_{\text{int}}$ that can be split in a part describing the noninteracting Fermi system,

$$\begin{aligned} \mathcal{S}_{\text{free}} = \int dr \left\{ \psi_{r,\uparrow}^\dagger \left(\frac{\partial}{\partial \tau} - \nabla_{\mathbf{r}}^2 - \mu_\uparrow - h_z \right) \psi_{r,\uparrow} \right. \\ + \psi_{r,\downarrow}^\dagger \left(\frac{\partial}{\partial \tau} - \nabla_{\mathbf{r}}^2 - \mu_\downarrow + h_z \right) \psi_{r,\downarrow} \\ \left. - \psi_{r,\uparrow}^\dagger \hat{h}_\perp^* \psi_{r,\downarrow} - \psi_{r,\downarrow}^\dagger \hat{h}_\perp \psi_{r,\uparrow} \right\}, \end{aligned} \quad (\text{A1})$$

where $r = \{\mathbf{r}, \tau\}$ and $\int dr = \int_0^\beta d\tau \int d\mathbf{r}$, and a part describing the interactions \mathcal{S}_{int} , which is given by Eq. (6) after introducing the Hubbard-Stratonovich fields. Performing the gauge transformation (7)–(9) leads to

$$\begin{aligned} \mathcal{S}_{\text{free}} = \int dr \left\{ -e^{i\phi} \tilde{\psi}_{r,\downarrow}^\dagger [\hat{h}_\perp + h_\perp(\phi_\uparrow)] \tilde{\psi}_{r,\uparrow} \right. \\ + \tilde{\psi}_{r,\downarrow}^\dagger \left(\frac{\partial}{\partial \tau} - \nabla_{\mathbf{r}}^2 - \mu_\downarrow + h_z + \xi(\phi_\downarrow) - \hat{\zeta}(\phi_\downarrow) \right) \tilde{\psi}_{r,\downarrow} \\ + \tilde{\psi}_{r,\uparrow}^\dagger \left(\frac{\partial}{\partial \tau} - \nabla_{\mathbf{r}}^2 - \mu_\uparrow - h_z + \xi(\phi_\uparrow) - \hat{\zeta}(\phi_\uparrow) \right) \tilde{\psi}_{r,\uparrow} \\ \left. - e^{-i\phi} \tilde{\psi}_{r,\uparrow}^\dagger [\hat{h}_\perp^* + h_\perp^*(\phi_\downarrow)] \tilde{\psi}_{r,\downarrow} \right\}, \end{aligned} \quad (\text{A2})$$

where we have introduced some additional notation:

$$\xi(\phi_s) = i \frac{\partial \phi_s}{\partial \tau} + (\nabla_{\mathbf{r}} \phi_s)^2, \quad (\text{A3})$$

$$\hat{\zeta}(\phi_s) = 2i(\nabla_{\mathbf{r}} \phi_s) \cdot \nabla_{\mathbf{r}}, \quad (\text{A4})$$

$$h_\perp(\phi_s) = 2i\alpha(\partial_x \phi_s) - 2\gamma(\partial_y \phi_s). \quad (\text{A5})$$

The interaction action \mathcal{S}_{int} [Eq. (6)] is left invariant by the spin-dependent gauge transformation.

Before making a Fourier transformation, we assume that the phase fields ϕ_s vary slowly in space and time with respect to the typical variations of the fermionic degrees of freedom. When that is the case, we can coarse grain the system according to the slow degrees of freedom ϕ_s . The fast variables $\tilde{\psi}_{\mathbf{r},\tau,s}$ are integrated out, assuming they are in local equilibrium.

To perform the integration over the fast fermionic degrees of freedom, the Fourier transform convention is used,

$$\psi_{k,s} = \frac{1}{\sqrt{\beta L^2}} \int dr e^{i(\omega_n \tau - \mathbf{k} \cdot \mathbf{r})} \tilde{\psi}_{\mathbf{r},\tau,s}, \quad (\text{A6})$$

where $k = (\mathbf{k}, i\omega_n)$, with $\omega_n = (2n+1)\pi/\beta$ the fermionic Matsubara frequencies with $n \in \mathbb{Z}$. The resulting action functional for the terms describing the noninteracting system is

$$\begin{aligned} \mathcal{S}_{\text{free}} = \int dr \sum_k \left\{ -e^{+i\phi} [h_\perp(\mathbf{k}) + h_\perp(\phi_\uparrow)] \psi_{k,\downarrow}^\dagger \psi_{k,\uparrow} \right. \\ + [-i\omega_n + \xi_{\mathbf{k}} + \xi(\phi_\uparrow) - h_z - \zeta_{\mathbf{k}}(\phi_\uparrow)] \psi_{k,\uparrow}^\dagger \psi_{k,\uparrow} \\ + [-i\omega_n + \xi_{\mathbf{k}} + \xi(\phi_\downarrow) + h_z - \zeta_{\mathbf{k}}(\phi_\downarrow)] \psi_{k,\downarrow}^\dagger \psi_{k,\downarrow} \\ \left. - e^{-i\phi} [h_\perp^*(\mathbf{k}) + h_\perp^*(\phi_\downarrow)] \psi_{k,\uparrow}^\dagger \psi_{k,\downarrow} \right\}. \end{aligned} \quad (\text{A7})$$

In this expression, we introduce again additional notation to keep the expressions somewhat compact:

$$\xi_{\mathbf{k}} = \mathbf{k}^2 - \mu, \quad (\text{A8})$$

$$\xi(\phi_s) = i \frac{\partial \phi_s}{\partial \tau} + (\nabla_{\mathbf{r}} \phi_s)^2, \quad (\text{A9})$$

$$\zeta_{\mathbf{k}}(\phi_s) = -2(\nabla_{\mathbf{r}} \phi_s) \cdot \mathbf{k}, \quad (\text{A10})$$

$$h_\perp(\mathbf{k}) = 2i\alpha k_x - 2\gamma k_y. \quad (\text{A11})$$

The interaction part of the action functional in turn transforms to

$$\mathcal{S}_{\text{int}} = \int dr \sum_k \{ \psi_{k,\uparrow}^\dagger \psi_{-k,\downarrow}^\dagger \Delta + \psi_{-k,\downarrow} \psi_{k,\uparrow} \Delta^* \} - \frac{\Delta \Delta^*}{g}. \quad (\text{A12})$$

Some remarks are in order. First, note that the Fourier transform was taken with respect to the fast variables, so the derivatives of the phase fields remain. Moreover, the integration over the imaginary-time and space dependence of the phase fields is still present, indicated by $\int dr = (\beta L^2)^{-1} \int d\mathbf{r} \int d\tau$, where L^2 is the area of the two-dimensional Fermi system. Second, we use $\mu = (\mu_\uparrow + \mu_\downarrow)/2$. If any spin imbalance $\zeta = (\mu_\uparrow - \mu_\downarrow)/2$ is present, its effect can be absorbed in $h_z + \zeta \rightarrow h_z$. Third, for the pair field, we assume that pair condensation is present in the $q = (\mathbf{q}, i\Omega_n) = \mathbf{0}$ state, setting $\Delta_q = |\Delta| \delta(\mathbf{q}) \delta_{n,0}$, with Ω_n the bosonic Matsubara frequencies for the pair field. From here onward, we treat $|\Delta|$ at the saddle-point level and take into account fluctuation effects generated only by the phase fields.

$$\mathbb{A}_+ = \begin{pmatrix} -i\omega_n + \xi_{\mathbf{k}} + \xi(\phi_\uparrow) - h_z - \zeta_{\mathbf{k}}(\phi_\uparrow) & -e^{-i\phi_-} [h_\perp^*(\mathbf{k}) + h_\perp^*(\phi_\downarrow)] \\ -e^{+i\phi_-} [h_\perp(\mathbf{k}) + h_\perp(\phi_\uparrow)] & -i\omega_n + \xi_{\mathbf{k}} + \xi(\phi_\downarrow) + h_z - \zeta_{\mathbf{k}}(\phi_\downarrow) \end{pmatrix}. \quad (\text{A16})$$

Similarly, the \mathbb{A}_* (hole-particle) block is obtained by anticommuting the fields and performing a parity transformation $(\mathbf{k}, i\omega_n) \rightarrow (-\mathbf{k}, -i\omega_n)$:

$$\mathbb{A}_* = \begin{pmatrix} -i\omega_n - \xi_{\mathbf{k}} - \xi(\phi_\uparrow) + h_z - \zeta_{\mathbf{k}}(\phi_\uparrow) & -e^{+i\phi_-} [h_\perp(\mathbf{k}) - h_\perp(\phi_\uparrow)] \\ -e^{-i\phi_-} [h_\perp^*(\mathbf{k}) - h_\perp^*(\phi_\downarrow)] & -i\omega_n - \xi_{\mathbf{k}} - \xi(\phi_\downarrow) - h_z - \zeta_{\mathbf{k}}(\phi_\downarrow) \end{pmatrix}. \quad (\text{A17})$$

Finally, \mathbb{B}_+ (\mathbb{B}_-) provides the particle-particle (hole-hole) terms, with $\mathbb{B}_- = -\mathbb{B}_+$. From Eq. (A12) it is clear that

$$\mathbb{B}_+ = \begin{pmatrix} 0 & \Delta \\ -\Delta & 0 \end{pmatrix}. \quad (\text{A18})$$

Using the anticommutation of fermionic field operators, we get additional terms that no longer depend on the fermionic fields. They are collected in

$$\mathcal{S}_x = \beta \sum_k \left\{ (-i\omega_n + \xi_{\mathbf{k}}) + \frac{1}{2} \int dr \sum_{s \in \{\uparrow, \downarrow\}} (\nabla_{\mathbf{r}} \phi_s)^2 \right\}, \quad (\text{A19})$$

and we need to keep these terms since they regularize the total action.

The action in Eq. (A14) is quadratic in the fermionic fields where \mathbb{C}_k has a block-diagonal form. The fermionic fields can then be easily integrated out, and the resulting effective action can be written down using the trace-logarithmic formula

$$\mathcal{S}_{\text{eff}} = -\frac{1}{2} \text{Tr}[\ln[\beta \mathbb{C}_k(\{\phi_\uparrow, \phi_\downarrow\})]] - \beta L^2 \frac{\Delta \Delta^*}{g} + \mathcal{S}_x. \quad (\text{A20})$$

This effective action for the phase fields is the same as in Eq. (11).

APPENDIX B: DERIVATION OF THE PHASE FLUCTUATION ACTION

To obtain the phase fluctuation action from \mathcal{S}_{eff} [Eqs. (A20) and (11)], a low-energy and long-wavelength expansion to

The action $\mathcal{S} = \mathcal{S}_{\text{free}} + \mathcal{S}_{\text{int}}$ is quadratic in the fermionic fields, and in reciprocal space it is block diagonal. To bring out this block-diagonal structure, we use Nambu spinors with the following ordering convention:

$$\eta_k^\dagger = (\psi_{k,\uparrow}^\dagger \quad \psi_{k,\downarrow}^\dagger \quad \psi_{-k,\uparrow} \quad \psi_{-k,\downarrow}). \quad (\text{A13})$$

Using this notation, the action functional can be written as

$$\mathcal{S} = \frac{1}{2} \int dr \sum_k \eta_k^\dagger \mathbb{C}_k \eta_k - \frac{\Delta \Delta^*}{g} + \mathcal{S}_x. \quad (\text{A14})$$

The action is diagonal in k . The factor $\frac{1}{2}$ appears to avoid double counting. The 4×4 inverse Green's function \mathbb{C}_k for the fermionic fields (more commonly denoted by $-\mathbb{G}_k^{-1}$) exhibits the substructure

$$\mathbb{C}_k = \begin{pmatrix} \mathbb{A}_+ & \mathbb{B}_+ \\ \mathbb{B}_- & \mathbb{A}_* \end{pmatrix} \quad (\text{A15})$$

with 2×2 blocks. The \mathbb{A}_+ (particle-hole) block can be read off from $\mathcal{S}_{\text{free}}$ [Eq. (A7)], keeping the usual order of operators:

Gaussian order in $(\phi_\uparrow, \phi_\downarrow)$ needs to be performed. The trace in Eq. (A20) above is written as

$$\begin{aligned} \text{Tr}[\ln[\beta \mathbb{C}_k(\{\phi_\uparrow, \phi_\downarrow\})]] &= \text{Tr}[\ln[\beta \mathbb{C}_k(\{0, 0\})]] \\ &+ \text{Tr}[\ln[\mathbb{I} + \mathbb{C}_k^{-1}(\{0, 0\}) \mathbb{D}_k(\{\phi_\uparrow, \phi_\downarrow\})]] \end{aligned} \quad (\text{B1})$$

to separate the saddle-point contribution $\mathbb{C}_k(\{0, 0\})$ from

$$\mathbb{D}_k(\{\phi_\uparrow, \phi_\downarrow\}) = \mathbb{C}_k(\{\phi_\uparrow, \phi_\downarrow\}) - \mathbb{C}_k(\{0, 0\}) \quad (\text{B2})$$

containing phase fluctuations. In turn, this allows us to write $\mathcal{S}_{\text{eff}} = \mathcal{S}_{\text{SP}} + \mathcal{S}_{\text{fl}}$, where the saddle-point action is

$$\begin{aligned} \mathcal{S}_{\text{SP}} &= -\frac{1}{2} \text{Tr}[\ln[\beta \mathbb{C}_k(\{0, 0\})]] + \beta \sum_k (-i\omega_n + \xi_{\mathbf{k}}) \\ &- \beta L^2 \frac{\Delta \Delta^*}{g} \end{aligned} \quad (\text{B3})$$

and the phase fluctuation action becomes

$$\begin{aligned} \mathcal{S}_{\text{fl}} &= -\frac{1}{2} \text{Tr}[\ln[\mathbb{C}_k^{-1}(\{0, 0\}) \mathbb{D}_k(\{\phi_\uparrow, \phi_\downarrow\})]] \\ &+ \frac{1}{4} \text{Tr}[\ln[(\mathbb{C}_k^{-1}(\{0, 0\}) \mathbb{D}_k(\{\phi_\uparrow, \phi_\downarrow\}))^2]], \end{aligned} \quad (\text{B4})$$

after an expansion the logarithm of the second term in Eq. (B1). The matrix for the phase fluctuations is

$$\mathbb{D}_k(\{\phi_\uparrow, \phi_\downarrow\}) = \begin{pmatrix} \epsilon_\uparrow^\dagger(\mathbf{k}) & [h_\uparrow^\downarrow(\mathbf{k})]^* & 0 & 0 \\ h_\uparrow^\dagger(\mathbf{k}) & \epsilon_\downarrow^\dagger(\mathbf{k}) & 0 & 0 \\ 0 & 0 & \epsilon_\uparrow^\dagger(\mathbf{k}) & h_\uparrow^\dagger(\mathbf{k}) \\ 0 & 0 & [h_\downarrow^\downarrow(\mathbf{k})]^* & \epsilon_\downarrow^\dagger(\mathbf{k}) \end{pmatrix}, \quad (\text{B5})$$

with matrix elements

$$\mathbf{e}_{\pm}^s(\mathbf{k}) = \pm \xi(\phi_s) - \zeta_{\mathbf{k}}(\phi_s), \quad (\text{B6})$$

$$\mathbf{h}_{\pm}^s(\mathbf{k}) = -e^{+i\phi_-}[h_{\perp}(\mathbf{k}) \pm h_{\perp}(\phi_s)]. \quad (\text{B7})$$

The inverse matrix $\mathbb{C}_k^{-1}(\{0, 0\})$ has only six independent components due to symmetry,

$$\mathbb{C}_k^{-1}(\{0, 0\}) = \frac{1}{D} \begin{pmatrix} A_{1,1} & A_{1,2} & A_{1,3} & A_{1,4} \\ A_{1,2}^* & A_{2,2} & -A_{1,4} & A_{2,4} \\ A_{1,3}^* & -A_{1,4}^* & -A_{1,1}^* & A_{1,2}^* \\ A_{1,4}^* & A_{2,4}^* & A_{1,2} & -A_{2,2}^* \end{pmatrix}, \quad (\text{B8})$$

where the determinant $D(\mathbf{k}, i\omega_n)$ of $\mathbb{C}_k(\{0, 0\})$ is

$$D(\mathbf{k}, i\omega_n) = (-i\omega_n + \epsilon_1)(-i\omega_n + \epsilon_2) \times (-i\omega_n - \epsilon_1)(-i\omega_n - \epsilon_2) \quad (\text{B9})$$

and the Bogoliubov energies in the presence of the spin-orbit coupling and Zeeman fields are

$$\epsilon_1 = \sqrt{E_{\mathbf{k}}^2 + |\mathbf{h}_{\text{eff}}(\mathbf{k})|^2 + 2\sqrt{E_{\mathbf{k}}^2|\mathbf{h}_{\text{eff}}(\mathbf{k})|^2 - |\Delta|^2|h_{\perp}(\mathbf{k})|^2}}, \quad (\text{B10})$$

$$\epsilon_2 = \sqrt{E_{\mathbf{k}}^2 + |\mathbf{h}_{\text{eff}}(\mathbf{k})|^2 - 2\sqrt{E_{\mathbf{k}}^2|\mathbf{h}_{\text{eff}}(\mathbf{k})|^2 - |\Delta|^2|h_{\perp}(\mathbf{k})|^2}}, \quad (\text{B11})$$

with $E_{\mathbf{k}}^2 = \xi_{\mathbf{k}}^2 + |\Delta|^2$ and $|\mathbf{h}_{\text{eff}}(\mathbf{k})|^2 = h_z^2 + |h_{\perp}(\mathbf{k})|^2$. The components of $\mathbb{C}_k^{-1}(\{0, 0\})$ are functions of $\{\mathbf{k}, i\omega_n\}$ and are given by

$$A_{1,1} = (-i\omega_n + \xi_{\mathbf{k}} + h_z)(-i\omega_n - \xi_{\mathbf{k}} + h_z) \times (-i\omega_n - \xi_{\mathbf{k}} - h_z) + |\Delta|^2(i\omega_n + \xi_{\mathbf{k}} + h_z) - (-i\omega_n + \xi_{\mathbf{k}} + h_z)|h_{\perp}(\mathbf{k})|^2, \quad (\text{B12})$$

$$A_{1,2} = h_{\perp}(\mathbf{k})|h_{\perp}(\mathbf{k})|^2 + |\Delta|^2 h_{\perp}(\mathbf{k}) + h_{\perp}^*(\mathbf{k}) \times (-i\omega_n - \xi_{\mathbf{k}} + h_z)(-i\omega_n - \xi_{\mathbf{k}} - h_z), \quad (\text{B13})$$

$$A_{1,3} = 2h_{\perp}(\mathbf{k})\Delta(\xi_{\mathbf{k}} + h_z), \quad (\text{B14})$$

$$A_{1,4} = |\Delta|^2\Delta + |h_{\perp}(\mathbf{k})|^2\Delta - \Delta(-i\omega_n + \xi_{\mathbf{k}} + h_z)(-i\omega_n - \xi_{\mathbf{k}} + h_z), \quad (\text{B15})$$

$$A_{2,2} = (-i\omega_n + \xi_{\mathbf{k}} - h_z)(-i\omega_n - \xi_{\mathbf{k}} + h_z) \times (-i\omega_n - \xi_{\mathbf{k}} - h_z) - |\Delta|^2(-i\omega_n - \xi_{\mathbf{k}} + h_z) - (-i\omega_n + \xi_{\mathbf{k}} - h_z)|h_{\perp}(\mathbf{k})|^2, \quad (\text{B16})$$

$$A_{2,4} = -2h_{\perp}^*(\mathbf{k})\Delta^*(\xi_{\mathbf{k}} - h_z). \quad (\text{B17})$$

These components are the building blocks for the analytical expressions of the phase stiffness and compressibility tensor listed in Appendix C. In the present Appendix, we focus on the resulting form of the fluctuation action

$$\mathcal{S}_{\text{fl}} = \frac{1}{2} \int dr (\kappa_{ss'} \partial_{\tau} \phi_s \partial_{\tau} \phi_{s'} + \rho_{ss'}^{\lambda\nu} \partial_{\lambda} \phi_s \partial_{\nu} \phi_{s'}), \quad (\text{B18})$$

after the traces are taken in Eq. (B4). Here s and s' are spin $\{\uparrow, \downarrow\}$ indices, ∂_{τ} is the partial derivative with respect to imaginary time τ , and ∂_{λ} and ∂_{ν} are the partial spatial derivatives with λ or ν being $\{x, y\}$. We use Einstein's summation convention of repeated indices. The tensor $\kappa_{ss'}$ is the spin-dependent compressibility and the tensor $\rho_{ss'}^{\lambda\nu}$ describes a spin-dependent phase stiffness connecting the same or different spatial directions. The quantum action is more transparent when written in terms of the phases ϕ_{\pm} of the U(1) charge sector and ϕ_{\pm} of the SU(2) spin sector. The resulting expression is

$$\mathcal{S}_{\text{fl}} = \frac{1}{2} \int dr (\kappa_{mn} \partial_{\tau} \phi_m \partial_{\tau} \phi_n + \rho_{mn}^{\lambda\nu} \partial_{\lambda} \phi_m \partial_{\nu} \phi_n), \quad (\text{B19})$$

where now the indices m and n take values $\{+, -\}$. The coefficient κ_{++} and the matrix $\rho_{++}^{\lambda\nu}$ now represent the compressibility and spin stiffness matrix for the U(1) charge sector, whereas κ_{--} and $\rho_{--}^{\lambda\nu}$ are their counterparts in the SU(2) spin sector. Finally, there are coefficients κ_{+-}, κ_{-+} and matrices $\rho_{+-}^{\lambda\nu}, \rho_{-+}^{\lambda\nu}$ that characterize the coupling between the U(1) and SU(2) sectors for compressibility and phase stiffness, respectively. In Appendix C we provide explicit expressions for κ_{mn} and $\rho_{mn}^{\lambda\nu}$ in the case of equal Rashba and Dresselhaus spin-orbit coupling, which is relevant for the present work focusing on ultracold fermions.

APPENDIX C: PHASE STIFFNESS AND COMPRESSIBILITY TENSORS

We have derived the components of the compressibility matrix κ_{mn} and the phase stiffness tensor $\rho_{mn}^{\lambda\nu}$ in general, but here we focus on the ERD case, deferring the general spin-orbit coupling (including the Rashba-only limit) to future work. In the ERD case, the fluctuation action expressed for the phase fields of the charge and spin sectors reads

$$\mathcal{S}_{\text{fl}}[\{\phi_{\pm}, \phi_{\pm}\}] = \frac{1}{2} \int d\tau \int dr \left[\bar{\eta}_{\mathbf{r},\tau}^{(\tau)} \begin{pmatrix} \kappa_{++} & \kappa_{+-} \\ \kappa_{+-} & \kappa_{--} \end{pmatrix} \eta_{\mathbf{r},\tau}^{(\tau)} + \bar{\eta}_{\mathbf{r},\tau}^{(\mathbf{r})} \begin{pmatrix} \rho_{++}^{xx} & 0 & \rho_{+-}^{xx} & 0 \\ 0 & \rho_{++}^{yy} & 0 & \rho_{+-}^{yy} \\ \rho_{+-}^{xx} & 0 & \rho_{--}^{xx} & 0 \\ 0 & \rho_{+-}^{yy} & 0 & \rho_{--}^{yy} \end{pmatrix} \eta_{\mathbf{r},\tau}^{(\mathbf{r})} \right], \quad (\text{C1})$$

where now we use the Nambu spinor notation for the spatial partial derivatives as

$$\bar{\eta}_{\mathbf{r},\tau}^{(\mathbf{r})} = (\partial_x \phi_{+} \quad \partial_y \phi_{+} \quad \partial_x \phi_{-} \quad \partial_y \phi_{-}) \quad (\text{C2})$$

and for the temporal partial derivatives as

$$\bar{\eta}_{\mathbf{r},\tau}^{(\tau)} = (\partial_{\tau} \phi_{+} \quad \partial_{\tau} \phi_{-}). \quad (\text{C3})$$

We express the phase stiffnesses and the compressibilities in terms of auxiliary functions built from the matrix elements of $\mathbb{C}_k^{-1}(\{0, 0\})$, given in Eqs. (B9) and (B12)–(B17). In terms of these functions, the compressibilities are

$$\kappa_{+-} = \frac{1}{4\beta L^2} \sum_{\mathbf{k}, i\omega_n} \frac{1}{[D(\mathbf{k}, i\omega_n)]^2} \left[A_{2,2}^2(\mathbf{k}, i\omega_n) - A_{1,1}^2(\mathbf{k}, i\omega_n) + |A_{1,3}(\mathbf{k}, i\omega_n)|^2 - |A_{2,4}(\mathbf{k}, i\omega_n)|^2 \right], \quad (\text{C4})$$

$$\begin{aligned} \kappa_{\pm\pm} = & \frac{1}{4\beta L^2} \sum_{\mathbf{k}, i\omega_n} \frac{1}{[D(\mathbf{k}, i\omega_n)]^2} [|A_{2,4}(\mathbf{k}, i\omega_n)|^2 + |A_{1,3}(\mathbf{k}, i\omega_n)|^2 - A_{2,2}^2(\mathbf{k}, i\omega_n) - A_{1,1}^2(\mathbf{k}, i\omega_n) \\ & \pm 2A_{1,4}^2(\mathbf{k}, i\omega_n) \mp 2A_{1,2}(\mathbf{k}, i\omega_n)A_{1,2}^*(\mathbf{k}, -i\omega_n)]. \end{aligned} \quad (\text{C5})$$

The phase stiffnesses are written as

$$\rho_{++}^{xx} = r_1^{\uparrow\uparrow(xx)} + r_1^{\downarrow\downarrow(xx)} + 2(r_1^{\uparrow\downarrow(xx)} + r_2^{\downarrow\downarrow(xx)} + r_2^{\uparrow\uparrow(xx)} + r_4^{\uparrow\uparrow(xx)} + r_4^{\downarrow\downarrow(xx)}) + r_6^{\uparrow\uparrow} + r_6^{\downarrow\downarrow}, \quad (\text{C6})$$

$$\rho_{--}^{xx} = r_1^{\uparrow\uparrow(xx)} + r_1^{\downarrow\downarrow(xx)} - 2(r_1^{\uparrow\downarrow(xx)} + r_2^{\downarrow\downarrow(xx)} - r_2^{\uparrow\uparrow(xx)}) + r_6^{\uparrow\uparrow} + r_6^{\downarrow\downarrow}, \quad (\text{C7})$$

$$\rho_{+-}^{xx} = r_1^{\uparrow\uparrow(xx)} - r_1^{\downarrow\downarrow(xx)} + r_4^{\uparrow\uparrow(xx)} - r_4^{\downarrow\downarrow(xx)} + r_6^{\uparrow\uparrow} - r_6^{\downarrow\downarrow}. \quad (\text{C8})$$

The expressions for ρ_{++}^{yy} , ρ_{--}^{yy} , and ρ_{+-}^{yy} can be found by substituting $xx \rightarrow yy$ in the expressions above. The auxiliary r functions are in turn listed below. The $r_1^{(xx)}$ functions are

$$r_1^{\uparrow\uparrow(xx)} = \frac{1}{\beta L^2} \sum_{\mathbf{k}, i\omega_n} \frac{1}{[D(\mathbf{k}, i\omega_n)]^2} [A_{1,1}^2(\mathbf{k}, i\omega_n) + |A_{1,3}(\mathbf{k}, i\omega_n)|^2] k_x^2, \quad (\text{C9})$$

$$r_1^{\downarrow\downarrow(xx)} = \frac{1}{\beta L^2} \sum_{\mathbf{k}, i\omega_n} \frac{1}{[D(\mathbf{k}, i\omega_n)]^2} [A_{2,2}^2(\mathbf{k}, i\omega_n) + |A_{2,4}(\mathbf{k}, i\omega_n)|^2] k_x^2, \quad (\text{C10})$$

$$r_1^{\uparrow\downarrow(xx)} = \frac{1}{\beta L^2} \sum_{\mathbf{k}, i\omega_n} \frac{1}{[D(\mathbf{k}, i\omega_n)]^2} [A_{1,4}^2(\mathbf{k}, i\omega_n) + A_{1,2}(\mathbf{k}, i\omega_n)A_{1,2}^*(\mathbf{k}, -i\omega_n)] k_x^2. \quad (\text{C11})$$

The corresponding r_1 functions with yy index are found by replacing k_x^2 by k_y^2 as the last factor in these expressions. For the functions r_2 we have

$$r_2^{\uparrow\downarrow(xx)} = \frac{v^2}{\beta L^2} \sum_{\mathbf{k}, i\omega_n} \frac{A_{1,1}(\mathbf{k}, i\omega_n)A_{2,2}(\mathbf{k}, i\omega_n) + |A_{1,4}(\mathbf{k}, i\omega_n)|^2}{[D(\mathbf{k}, i\omega_n)]^2}, \quad (\text{C12})$$

$$r_2^{\uparrow\uparrow(xx)} = \frac{v^2}{\beta L^2} \sum_{\mathbf{k}, i\omega_n} \frac{A_{1,2}^2(\mathbf{k}, i\omega_n) - A_{1,3}(\mathbf{k}, i\omega_n)A_{2,4}^*(\mathbf{k}, i\omega_n)}{[D(\mathbf{k}, i\omega_n)]^2}, \quad (\text{C13})$$

and $r_2^{\uparrow\downarrow(yy)} = 0 = r_2^{\uparrow\uparrow(yy)}$. The functions r_4 are given by

$$r_4^{\uparrow\downarrow(xx)} = \frac{-4v^2}{\beta L^2} \sum_{\mathbf{k}, i\omega_n} \frac{A_{1,2}(\mathbf{k}, i\omega_n)A_{2,2}(\mathbf{k}, i\omega_n) + A_{2,4}(\mathbf{k}, i\omega_n)A_{2,4}^*(\mathbf{k}, i\omega_n)}{[D(\mathbf{k}, i\omega_n)]^2 h_{\perp}(\mathbf{k})} k_x^2, \quad (\text{C14})$$

$$r_4^{\uparrow\uparrow(xx)} = \frac{-4v^2}{\beta L^2} \sum_{\mathbf{k}, i\omega_n} \frac{A_{1,1}(\mathbf{k}, i\omega_n)A_{1,2}(\mathbf{k}, i\omega_n) - A_{1,3}(\mathbf{k}, i\omega_n)A_{1,4}(\mathbf{k}, i\omega_n)}{[D(\mathbf{k}, i\omega_n)]^2 h_{\perp}(\mathbf{k})} k_x^2, \quad (\text{C15})$$

and $r_4^{\uparrow\downarrow(yy)} = 0 = r_4^{\uparrow\uparrow(yy)}$. Finally, the r_6 functions are given by

$$r_6^{\uparrow\uparrow} = \frac{1}{2\beta L^2} \sum_{\mathbf{k}, i\omega_n} \left(\frac{\beta}{2} - \frac{A_{1,1}(\mathbf{k}, i\omega_n)}{D(\mathbf{k}, i\omega_n)} \right), \quad (\text{C16})$$

$$r_6^{\downarrow\downarrow} = \frac{1}{2\beta L^2} \sum_{\mathbf{k}, i\omega_n} \left(\frac{\beta}{2} - \frac{A_{2,2}(\mathbf{k}, i\omega_n)}{D(\mathbf{k}, i\omega_n)} \right) \quad (\text{C17})$$

and are independent of the spatial indices.

- [1] G. E. Volovik, *Exotic Properties of Superfluid ^3He* (World Scientific, Singapore, 1992).
 [2] N. Read and D. Green, Paired states of fermions in two dimensions with breaking of parity and time-reversal symmetries and the fractional quantum Hall effect, *Phys. Rev. B* **61**, 10267 (2000).
 [3] R. D. Duncan and C. A. R. Sá de Melo, Thermodynamic properties in the evolution from BCS to Bose-Einstein condensation

for a d -wave superconductor at low temperatures, *Phys. Rev. B* **62**, 9675 (2000).

- [4] M. Gong, S. Tewari, and C. Zhang, BCS-BEC Crossover and Topological Phase Transition in 3D Spin-Orbit Coupled Degenerate Fermi Gases, *Phys. Rev. Lett.* **107**, 195303 (2011).
 [5] H. Hu, L. Jiang, X.-J. Liu, and H. Pu, Probing Anisotropic Superfluidity in Atomic Fermi Gases with Rashba Spin-Orbit Coupling, *Phys. Rev. Lett.* **107**, 195304 (2011).

- [6] Z.-Q. Yu and H. Zhai, Spin-Orbit Coupled Fermi Gases across a Feshbach Resonance, *Phys. Rev. Lett.* **107**, 195305 (2011).
- [7] L. Han and C. A. R. Sá de Melo, Evolution from BCS to BEC superfluidity in the presence of spin-orbit coupling, *Phys. Rev. A* **85**, 011606(R) (2012).
- [8] K. Seo, L. Han, and C. A. R. Sá de Melo, Emergence of Majorana and Dirac Particles in Ultracold Fermions via Tunable Interactions, Spin-Orbit Effects and Zeeman fields, *Phys. Rev. Lett.* **109**, 105303 (2012).
- [9] A. P. Schnyder, S. Ryu, A. Furusaki, and A. W. W. Ludwig, Classification of topological insulators and superconductors in three spatial dimensions, *Phys. Rev. B* **78**, 195125 (2008).
- [10] S. Ryu, A. P. Schnyder, A. Furusaki, and A. W. W. Ludwig, Topological insulators and superconductors: Ten-fold way and dimensional hierarchy, *New J. Phys.* **12**, 065010 (2010).
- [11] A. Altland and M. R. Zimbauer, Nonstandard symmetry classes in mesoscopic normal-superconducting hybrid structures, *Phys. Rev. B* **55**, 1142 (1997).
- [12] L. P. Gor'kov and E. I. Rashba, Superconducting 2D System with Lifted Spin Degeneracy: Mixed Singlet-Triplet State, *Phys. Rev. Lett.* **87**, 037004 (2001).
- [13] S. K. Yip, Two-dimensional superconductivity with strong spin-orbit interaction, *Phys. Rev. B* **65**, 144508 (2002).
- [14] P. A. Frigeri, D. F. Agterberg, A. Koga, and M. Sigrist, Superconductivity without Inversion Symmetry: MnSi versus CePt₃Si, *Phys. Rev. Lett.* **92**, 097001 (2004).
- [15] V. P. Mineev, Paramagnetic limit of superconductivity in a crystal without an inversion center, *Phys. Rev. B* **71**, 012509 (2005).
- [16] P. Wang, Z. Q. Yu, Z. Fu, J. Miao, L. Huang, S. Chai, H. Zhai, and J. Zhang, Spin-Orbit Coupled Degenerate Fermi Gases, *Phys. Rev. Lett.* **109**, 095301 (2012).
- [17] L. W. Cheuk, A. T. Sommer, Z. Hadzibabic, T. Yefsah, W. S. Bakr, and M. W. Zwierlein, Spin-Injection Spectroscopy of a Spin-Orbit Coupled Fermi Gas, *Phys. Rev. Lett.* **109**, 095302 (2012).
- [18] R. A. Williams, M. C. Beeler, L. J. LeBlanc, K. Jiménez-García, and I. B. Spielman, Raman-Induced Interactions in a Single-Component Fermi Gas Near an *s*-Wave Feshbach Resonance, *Phys. Rev. Lett.* **111**, 095301 (2013).
- [19] Z. Fu, L. Huang, Z. Meng, P. Wang, L. Zhang, S. Zhang, H. Zhai, P. Zhang, and J. Zhang, Production of Feshbach molecules induced by spin-orbit coupling in Fermi gases, *Nat. Phys.* **10**, 110 (2014).
- [20] C. A. R. Sá de Melo, M. Randeria, and J. R. Engelbrecht, Crossover from BCS to Bose Superconductivity: Transition Temperature and Time-Dependent Ginzburg-Landau Theory, *Phys. Rev. Lett.* **71**, 3202 (1993).
- [21] J. P. Vyasanakere, S. Zhang, and V. B. Shenoy, BCS-BEC crossover induced by a synthetic non-Abelian gauge field, *Phys. Rev. B* **84**, 014512 (2011).
- [22] S. S. Botelho and C. A. R. Sá de Melo, Vortex-Antivortex Lattice in Ultracold Fermionic Gases, *Phys. Rev. Lett.* **96**, 040404 (2006).
- [23] J. Tempere, S. N. Klimin, and J. T. Devreese, Effect of population imbalance on the Berezinskii-Kosterlitz-Thouless phase transition in a superfluid Fermi gas, *Phys. Rev. A* **79**, 053637 (2009).
- [24] L. He and Z.-G. Huang, BCS-BEC Crossover in 2D Fermi Gases with Rashba Spin-Orbit Coupling, *Phys. Rev. Lett.* **108**, 145302 (2012).
- [25] J. P. A. Devreese, J. Tempere, and C. A. R. Sá de Melo, Effects of Spin-Orbit Coupling on the Berezinskii-Kosterlitz-Thouless Transition and the Vortex-Antivortex Structure in Two-Dimensional Fermi Gases, *Phys. Rev. Lett.* **113**, 165304 (2014).
- [26] J. P. A. Devreese, J. Tempere, and C. A. R. Sá de Melo, Quantum phase transitions and Berezinskii-Kosterlitz-Thouless temperature in a two-dimensional spin-orbit-coupled Fermi gas, *Phys. Rev. A* **92**, 043618 (2015).
- [27] V. L. Berezinskii, Destruction of long-range order in one-dimensional and two-dimensional systems with a continuous symmetry group. II. Quantum systems, *Sov. Phys. JETP* **32**, 493 (1971).
- [28] J. M. Kosterlitz and D. J. Thouless, Long range order and metastability in two dimensional solids and superfluids, *J. Phys. C* **5**, L124 (1972).
- [29] Y. A. Byshkov and E. I. Rashba, Oscillatory effects and the magnetic-susceptibility of carriers in inversion-layers, *J. Phys. C* **17**, 6039 (1984).
- [30] G. Dresselhaus, Spin-orbit coupling effects in zinc blende structures, *Phys. Rev.* **100**, 580 (1955).
- [31] S. Nascimbene, N. Navon, S. Pilati, F. Chevy, S. Giorgini, A. Georges, and C. Salomon, Fermi-Liquid Behavior of the Normal Phase of a Strongly Interacting Gas of Cold Atoms, *Phys. Rev. Lett.* **106**, 215303 (2011).
- [32] C. Sanner, E. J. Su, A. Keshet, W. Huang, J. Gillen, R. Gommers, and W. Ketterle, Speckle Imaging of Spin Fluctuations in a Strongly Interacting Fermi Gas, *Phys. Rev. Lett.* **106**, 010402 (2011).
- [33] Y. Long, F. Xiong, and C. V. Parker, Spin Susceptibility above the Superfluid Onset in Ultracold Fermi Gases, *Phys. Rev. Lett.* **126**, 153402 (2021).
- [34] S. R. Muniz, D. S. Naik, M. Bhattacharya, and C. Raman, Dynamics of rotating Bose-Einstein condensates probed by Bragg scattering, *Math. Comput. Simul.* **74**, 397 (2007).
- [35] P. B. Blakie and R. J. Ballagh, Spatially Selective Bragg Scattering: A Signature for Vortices in Bose-Einstein Condensates, *Phys. Rev. Lett.* **86**, 3930 (2001).
- [36] F. Chevy, K. W. Madison, V. Bretin, and J. Dalibard, Interferometric detection of a single vortex in a dilute Bose-Einstein condensate, *Phys. Rev. A* **64**, 031601(R) (2001).
- [37] Z. Hadzibabic, P. Krüger, M. Cheneau, B. Battelier, and J. Dalibard, Berezinskii-Kosterlitz-Thouless crossover in a trapped atomic gas, *Nature (London)* **441**, 1118 (2006).
- [38] P. Cladé, C. Ryu, A. Ramanathan, K. Helmerson, and W. D. Phillips, Observation of a 2D Bose Gas: From Thermal to Quasicondensate to Superfluid, *Phys. Rev. Lett.* **102**, 170401 (2009).
- [39] M. R. Matthews, B. P. Anderson, P. C. Haljan, D. S. Hall, C. E. Wieman, and E. A. Cornell, Vortices in a Bose-Einstein Condensate, *Phys. Rev. Lett.* **83**, 2498 (1999).